0013-7227/02/$15.00/0
Printed in U.S.A.

The Journal of Clinical Endocrinology & Metabolism 87(3):1223–1232

Resveratrol Induces Apoptosis in Thyroid Cancer Cell Lines via a MAPK- and p53-Dependent Mechanism

AI SHIH, FAITH B. DAVIS, HUNG-YUN LIN, AND PAUL J. DAVIS

Medical Research Service, Stratton Veterans Affairs Medical Center (A.S., F.B.D., H.-Y.L., P.J.D.), the Clinical Research Institute, Albany Medical College (F.B.D., P.J.D.), and the Wadsworth Center, New York State Department of Health (P.J.D.), Albany, New York 12208

Two papillary thyroid carcinoma (PTC) and two follicular thyroid carcinoma (FTC) cell lines treated with resveratrol (RV), 1–10 μM, showed activation and nuclear translocation of MAPK (extracellular signal-regulated kinase 1/2). Cellular abundance of the oncogene suppressor protein p53, serine phosphorylation of p53, and abundance of c-*fos*, c-*jun*, and *p21* mRNAs were also increased by RV. Inhibition of the MAPK pathway by either H-*ras* antisense transfection or PD 98059, an MAPK kinase inhibitor, blocked these RV-induced effects. Addition of pifithrin-α, a specific inhibitor of p53, or transfection of p53 antisense oligonucleotides caused decreased RV-induced p53 and *p21* expression in PTC and FTC cells. Studies of nucleosome levels estimated by ELISA and of DNA fragmentation showed that RV induced apoptosis in both papillary and follicular thyroid cancer cell lines; these effects were inhibited by pifithrin-α and by p53 antisense oligonucleotide transfection. PD 98059 and H-*ras* antisense transfection also blocked induction of apoptosis by RV. Thus, RV acts via a Ras-MAPK kinase-MAPK signal transduction pathway to increase p53 expression, serine phosphorylation of p53, and p53-dependent apoptosis in PTC and FTC cell lines. (*J Clin Endocrinol Metab* 87: 1223–1232, 2002)

RESVERATROL IS A phytoalexin that occurs naturally in grapes and several medicinal plants (1, 2). It has chemopreventive activity in mouse models of mammary gland and skin cancer (2) and has been reported to have other antitumor effects (2–4). The mechanism of the antitumor effects of resveratrol (RV) is not well understood, but in some tumor cell models may involve induction of apoptosis (3, 5, 6). Apoptosis is an intrinsic protective mechanism (7, 8) by which genetically damaged cells or excessive numbers of cells inappropriately induced by a mitotic stimulus may be eliminated (9). A potential strategy of cancer management is the pharmacologic induction of apoptosis in established cancer cells.

p53 is an oncogene suppressor protein present at low levels in the normal cell (10). In response to stresses such as DNA damage (10), levels of cellular p53 protein rise; this increase in p53 appears to result from a posttranslational mechanism that stabilizes the protein (11). When specifically phosphorylated at several serines, p53 promotes apoptosis (12). p53 is a substrate for serine kinases such as Jun N-terminal kinase (JNK) (13), p38 kinase, and extracellular signal-regulated kinases 1 and 2 (ERK1/2) (14). p53 alone, or in conjunction with other proteins such as c-Jun (15), is involved in induction of apoptosis by anticancer drugs directed against cancers of the prostate (15), lung (15), breast (16), and thyroid gland (17).

MAPK (ERK1/2), an inducible component of normal cellular signal transduction processes, has been shown to be constitutively activated (phosphorylated) in several cancer cell lines (18–20). In contrast to such constitutive activity of ERK1/2, transient activation of the kinases may contribute to induction of apoptosis (21, 22). ERK1/2 is also an upstream regulator of the p53 response to DNA damage caused by the apoptosis-inducing drug cisplatin (23).

In the present studies of established human papillary (PTC) and follicular thyroid carcinoma (FTC) cell lines, we found that exposure of cells to RV revealed activation of MAPK. MAPK activation was associated with a subsequent increase in abundance of nuclear p53 protein that was shown to be phosphorylated at serines 6 and 15 in FTC and serine 15 in PTC cells. These changes in cellular MAPK and p53 were associated with induction of apoptosis. We have recently reported that p53 is a substrate for activated MAPK (24).

Materials and Methods

Cell lines

Two human PTC cell lines (BHP 2–7 and BHP 18–21), generously provided by Dr. J. M. Hershman (West Los Angeles Veterans Affairs Medical Center, Los Angeles, CA) were studied. Two FTC cell lines (FTC 236 and FTC 238) were kindly provided by Dr. Orlo Clark (University of California at San Francisco-Mt. Zion Medical Center, San Francisco, CA) with permission of Dr. Peter Goretski. PTC cells were cultured in Roswell Park Memorial Institute 1640 medium, and FTC cells in 50% DMEM/50% Ham's F-12 plus 10 mU/ml of TSH (Sigma, St. Louis, MO); media were supplemented with 10% FBS, and cells were maintained in 5% CO_2 at 37 C. All cell cultures were incubated with fresh media containing 0.25% hormone-depleted FBS for 2 d before study.

Cell fractionation

After treatment with RV and/or other agents for indicated times, the cells were washed with ice-cold PBS and lysed in hypotonic buffer (20 mM HEPES [pH 7.9], 10 mM KCl, 0.1 mM Na_3VO_4, 1 mM EDTA, 10% glycerol, 1 mM PMSF, 3 μg aprotinin/ml, 1 mg pepstatin/ml, 20 mM

Abbreviations: AS, Antisense oligonucleotide; DTT, dithiothreitol; ERK1 and ERK2, extracellular signal-regulated kinases 1 and 2; FTC, follicular thyroid carcinoma; GAPDH, glyceraldehyde-3-phosphate dehydrogenase; JNK, Jun N-terminal kinase; MEK, MAPK kinase; PD, PD98059; PFT-α, pifithrin-α; pMAPK, phosphorylated MAPK; PTC, papillary thyroid carcinoma; RV, resveratrol; Scr, scrambled oligonucleotide.

NaF, and 1 mM DTT), with 0.2% NP-40. Lysis occurred over 10 min with cells on ice. After centrifugation at 4 C for 1 min at 13,000 rpm, the supernatants were collected as cytosol. Nuclear extracts were prepared by resuspension of the crude nuclei in high salt buffer (hypotonic buffer to which was added 20% glycerol and 420 mM NaCl) at 4 C, with rocking for 1 h. The nucleoprotein-containing supernatants were collected after centrifugation at 4 C for 10 min at 13,000 rpm.

Immunoblotting

Proteins were separated by discontinuous SDS-PAGE (9%) and transferred by electroblotting to Immobilon membranes (Millipore Corp., Bedford, MA). After blocking with 5% milk in Tris-buffered saline containing 0.1% Tween, membranes were incubated overnight with one of various antibodies including rabbit polyclonal antiphosphorylated MAPK (ERK1 and ERK2) (New England Biolabs, Inc. [NEB], Beverly, MA), anti-serine-15- or anti-serine-6-phosphorylated p53 (NEB), anti-p21 (Santa Cruz Biotechnology, Inc., Santa Cruz, CA), anti-c-Fos (Santa Cruz Biotechnology, Inc.), or mouse monoclonal anti-c-Jun or anti-p53 (Santa Cruz Biotechnology, Inc.). The secondary antibody was either goat anti-rabbit IgG (1:1000) or rabbit anti-mouse IgG (1:1000) (DAKO Corp., Carpinteria, CA). Immunoblotted proteins were visualized by chemiluminescence and scanned for illustration (BioImage, Millipore Corp.).

Transfection of H-ras and p53 antisense oligonucleotides

Using a technique previously described by our laboratory (24), thyroid cancer cells were transfected with 7.5 μg of either *H-ras* antisense or scrambled oligonucleotide (25) or with 5.0 μg of either p53 antisense or scrambled oligonucleotide (26) (Operon Technologies, Alameda, CA) in the presence of LIPOFECTAMINE PLUS reagent (Life Technologies, Inc., Grand Island, NY) for 6 h. The medium was then replaced with fresh medium containing 0.25% thyroid hormone-depleted FBS (24) and cells were treated with or without 10 μM RV for 48 h.

Determination of c-fos, c-jun, p21, and GAPDH mRNAs

Total RNA was isolated as described previously (27). First strand cDNAs were synthesized from 1 μg of total RNA using oligodeoxythymidine and Avian Myeloblastosis Virus Reverse Transcriptase (Promega Corp., Madison, WI). First-strand cDNA templates were amplified for *GAPDH*, c-*fos*, c-*jun*, and *p21* by PCR using a hot start (Ampliwas, Perkin-Elmer Corp., Foster City, CA). Primer sequences used were as described by Irving *et al.* (28). The PCR cycle consisted of an initial step of 95 C for 3 min, followed by 94 C for 1 min, 55 C for 1 min, 72 C for 1 min for 25 cycles, and a final cycle of 72 C for 8 min. PCR products normalized to give equal signals from GAPDH were subjected to electrophoresis in 2% agarose gel containing 0.5 μg/ml of ethidium bromide. Gels were visualized under UV light and photographed with Polaroid film (Polaroid Co. Cambridge, MA). Photographs were scanned for illustration.

Nucleosome ELISA assay for detection of apoptosis

Cells were harvested and washed with PBS. Nucleosome ELISAs were carried out according to the protocol provided by Oncogene Research Products (Cambridge, MA).

DNA fragmentation

Total genomic DNA extraction followed the protocol of the SUICIDE-TRACK DNA LADDER ISOLATION KIT (Oncogene). DNA electrophoresis was performed in 1.5% agarose gels containing 0.5 μg/ml of ethidium bromide. Gels were visualized under UV light and photographed with Polaroid film. Photographs were scanned as indicated above.

Using the methods described above, all experiments reported were carried out at least three times with comparable results.

Results

Activated MAPK in thyroid cancer cell lines

With the addition to BHP 18–21 and FTC 236 cells of RV, 0.1 to 100 μM, for 4 and 24 h, nuclear extracts revealed the presence of activated MAPK, detected with antiphospho-MAPK that recognized both ERK1 and ERK2 isoforms (Fig. 1A). There was concentration-dependent activation of MAPK with 0.1–100 μM RV at 4 h and with 0.1–10 μM RV at 24 h. However, less activated MAPK was found after treat-

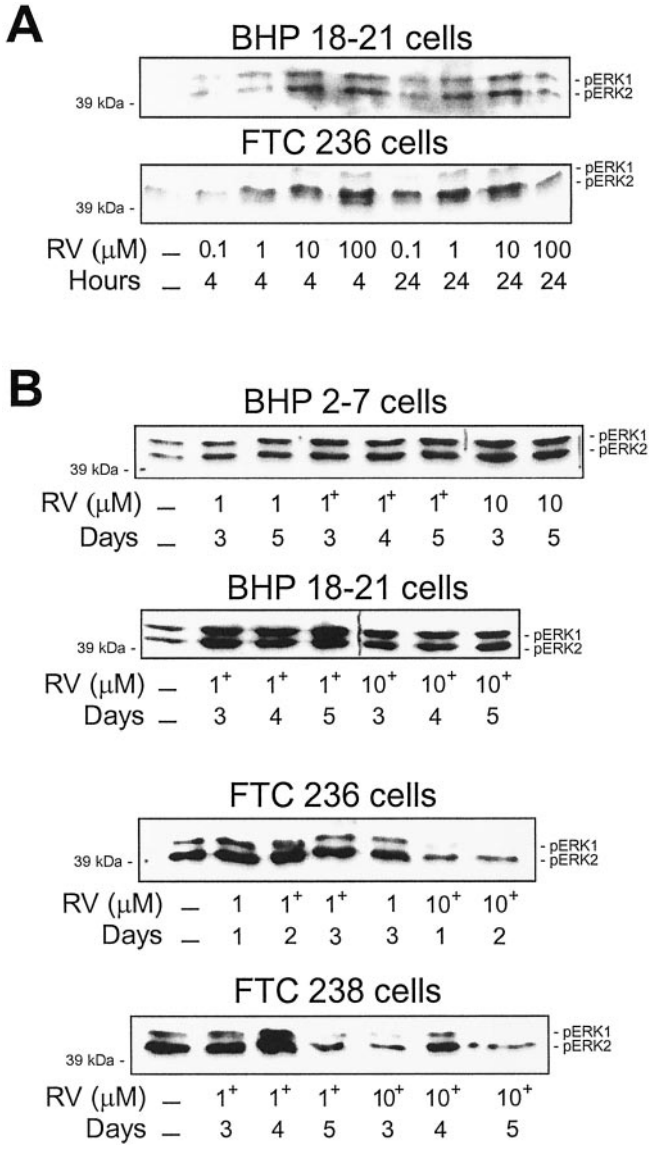

FIG. 1. Activation of MAPK (ERK1/2) by RV in four thyroid carcinoma cell lines. A, Dose-response study over 4 and 24 h of RV-induced MAPK (ERK1/2) activation in nuclei of BHP 18–21 and FTC 236 cells, using an antibody to tyrosine-threonine-phosphorylated ERK1 and ERK2 (pERK1/2). These two cell lines showed little nuclear ERK1 and ERK2 isoforms in the absence of RV over a 24-h period (lanes at *far left*). There was increased MAPK activation in both cell lines after 4 and 24 h of RV treatment (0.1–100 μM). B, BHP 2–7 and BHP 18–21 cells showed minimal phosphorylation and nuclear accumulation of ERKs 1 and 2 in cells incubated for 5 d in the absence of RV (lanes at *left*). Cells were exposed to RV (1 or 10 μM) for 3–5 d, and media for certain samples were replenished with RV daily (indicated by [+]), thus enhancing the RV effect. RV treatment caused increases in nuclear ERKs 1/2 in 3–5 d with both concentrations. FTC 236 and FTC 238 cells also showed activation of ERKs 1/2 (lanes at *left*) after 5 d in the absence of RV. In these cell lines, 1–4 d of 1 μM RV treatment caused a further increase in ERK1/2 activation.

ment with 100 μM RV for 24 h. This was attributed to induction by RV of apoptosis at 24 h (results not shown). The pattern of activation of MAPK induced by RV showed some variation among thyroid cancer cell lines during longer time periods. In the absence of RV, some activation of nuclear MAPK was detected after 3–5 d in cultures of papillary and follicular thyroid cancer cell lines (Fig. 1B). For example, there was a sustained activated MAPK response to RV for 5 d (1 or 10 μM) in BHP 2–7 and BHP 18–21 cells, but activated MAPK was decreased at 5 d in FTC 238 cells (RV, 1–10 μM). In FTC 236 cells, treatment with 10 μM RV, in contrast to 1 μM, resulted in almost complete disappearance of activated MAPK at 1 and 2 d. As indicated above, this finding is attributed to the susceptibility of the cells to RV-induced apoptosis.

p53, c-jun, c-fos, and p21 mRNA and gene products in thyroid cancer cells after RV treatment

In BHP 2–7 cells treated with RV, there was increased abundance of p53 protein (Fig. 2A). RV at 10 μM was more effective than the phytoalexin at 1 μM. RV also caused accumulation of p21, an inhibitor of cyclin-dependent protein kinase activity (29), after 3–5 d of treatment, and c-Fos and c-Jun proteins were similarly increased (Fig. 2A). Using RT-PCR, we detected increased abundance of c-*fos* and c-*jun* mRNAs in BHP 2–7 cells treated with 1 μM RV (Fig. 2B).

In BHP 18–21 cells, 10 μM RV caused increased cell content of p53 and serine 15 phosphorylation of p53 at 3–5 d (Fig. 3A). p21 content was also increased in cells after 3–5 d of treatment with 10 μM RV, and c-Fos content increased with 1 and 10 μM RV (Fig. 3A). Increases in *p53*, c-*fos*, and *p21* mRNAs in RV-treated cells were seen, particularly after 3 d, with both concentrations (Fig. 3B).

Similar studies were also conducted in follicular thyroid cancer cells (Fig. 4). RV-induced increases in p53 and serine-15-phosphorylated p53 were seen in FTC 236 cells with 1 or 10 μM RV, whereas in FTC 238 cells increases in p53 and c-Fos were seen particularly with 1 μM RV (Fig. 4A). Treatment of cells with RV increased *p53* and *p21* mRNA levels in both FTC 236 and FTC 238 cells, and c-*fos* mRNA in FTC 236 cells (Fig. 4B).

The role of p53 in p21 expression induced by RV in thyroid cancer cells

To study whether the increase in *p21* mRNA in RV-treated thyroid cancer cells is p53-dependent, PTC and FTC cells were exposed to 10 μM RV in the presence or absence of 20 μM PFT-α, a specific p53 inhibitor (30). Total p53 accumulation and serine 15 phosphorylation of p53 were reduced by PFT-α in both PTC cell lines (Fig. 5A, lanes 4). The abundance

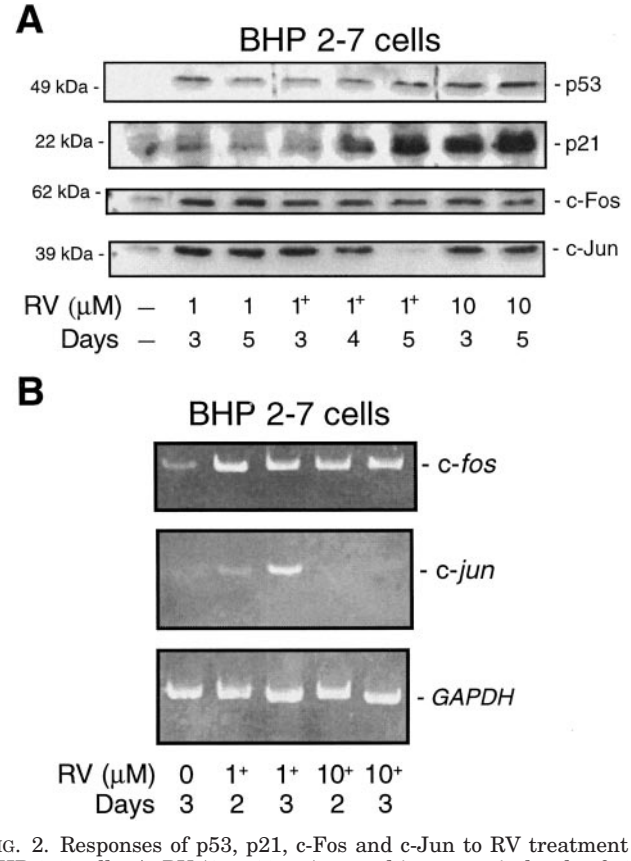

FIG. 2. Responses of p53, p21, c-Fos and c-Jun to RV treatment of BHP 2–7 cells. A, RV (1 or 10 μM) caused increases in levels of p53, p21, c-Fos, and c-Jun proteins, measured by immunoblot, in 3–5 d. B, RV (1 μM) caused increases in 2–3 d in c-*fos* and c-*jun* mRNAs, compared with *GAPDH* levels, while with 10 μM RV for 2–3 d less c-*fos* and c-*jun* were seen, suggesting more rapid turnover of mRNA.

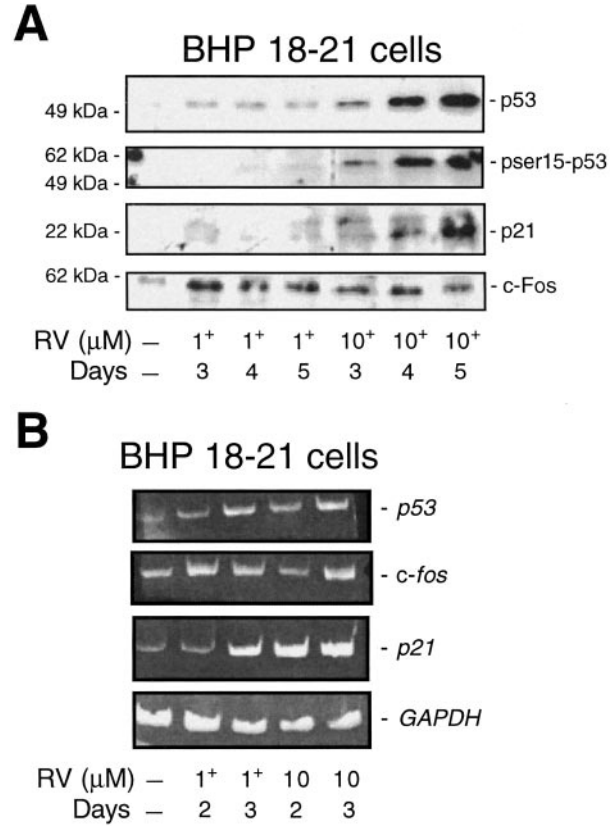

FIG. 3. Response of BHP 18–21 cells to RV treatment. A, RV induced increases in levels of p53, serine-15-phosphorylated p53 (pser15-p53), p21, and c-Fos proteins, measured by immunoblot, in 3–5 d. B, RV treatment increased levels of *p53*, c-*fos*, and *p21* mRNAs when compared with *GAPDH* levels.

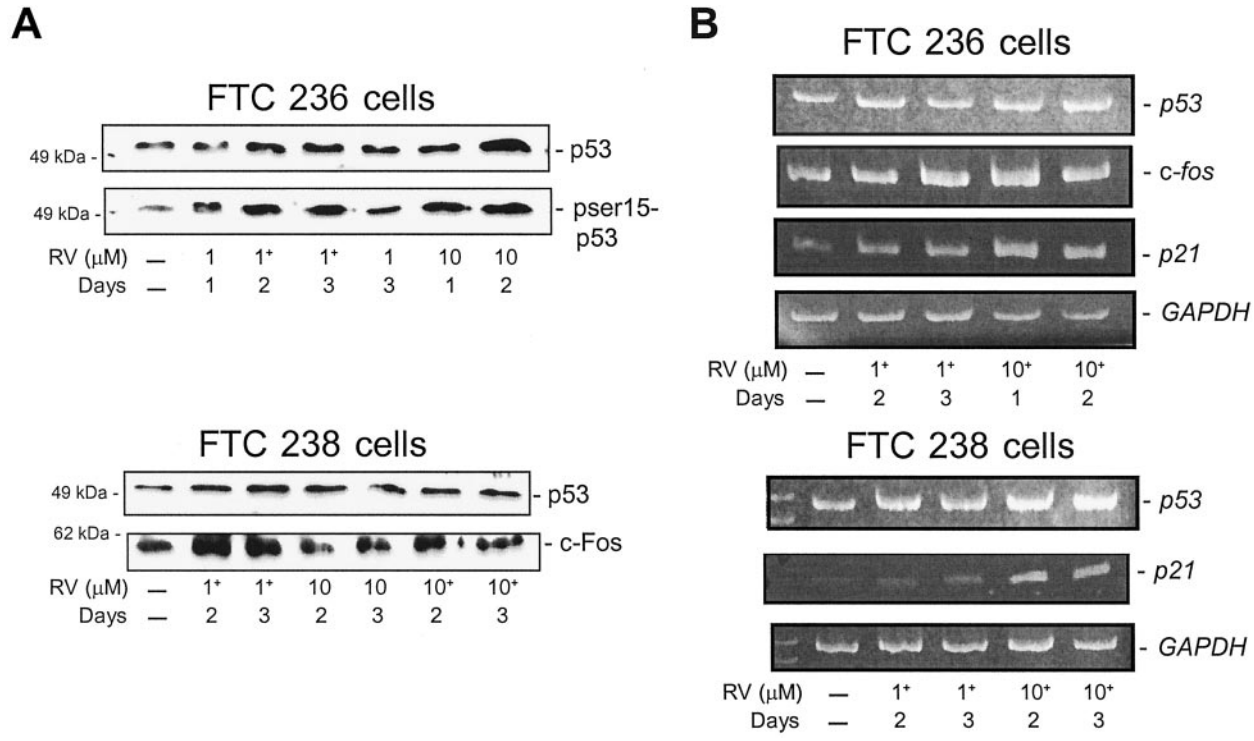

FIG. 4. Results of RV treatment in FTC 236 and FTC 238 cells. A, RV caused increases in nuclear levels of p53 and serine-15-phosphorylated p53 in FTC 236 cells, and of p53 and c-Fos in FTC 238 cells in 1–3 d. B, RV increased *p53*, c-*fos* and *p21* mRNA in FTC 236 cells, and *p53* and *p21* mRNA in FTC 238 cells.

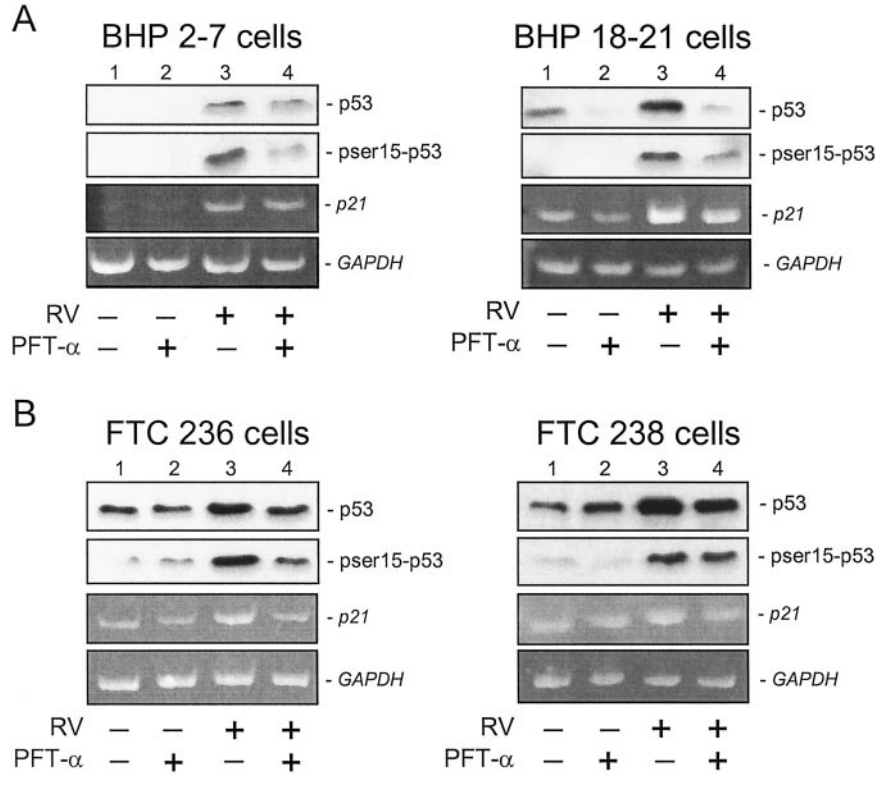

FIG. 5. Effect of pifithrin-α (PFT-α) on the phosphorylation of p53 and abundance of *p21* mRNA induced by RV. A, RV treatment (10 μM, 2 d) of BHP 2–7 and BHP 18–21 cells caused nuclear accumulation of p53, serine 15-phosphorylated p53 (pser15-p53) and *p21* mRNA (lanes 3). This RV effect was blocked by a specific p53 inhibitor, pifithrin-α (PFT-α, 20 μM) in both BHP 2–7 and BHP 18–21 cells (lanes 4). B, 20 μM PFT-α inhibited the same RV-induced effects in FTC 236 and FTC 238 cells.

of *p21* mRNA decreased in cells treated with RV and PFT-α, compared with levels in cells treated with RV alone, indicating a reduction in p53-dependent *p21* gene expression in both PTC cell lines (Fig. 5A). Similar results also were observed in two FTC cell lines (Fig. 5B). We also used *p53* antisense oligonucleotide transfection to decrease p53 con-

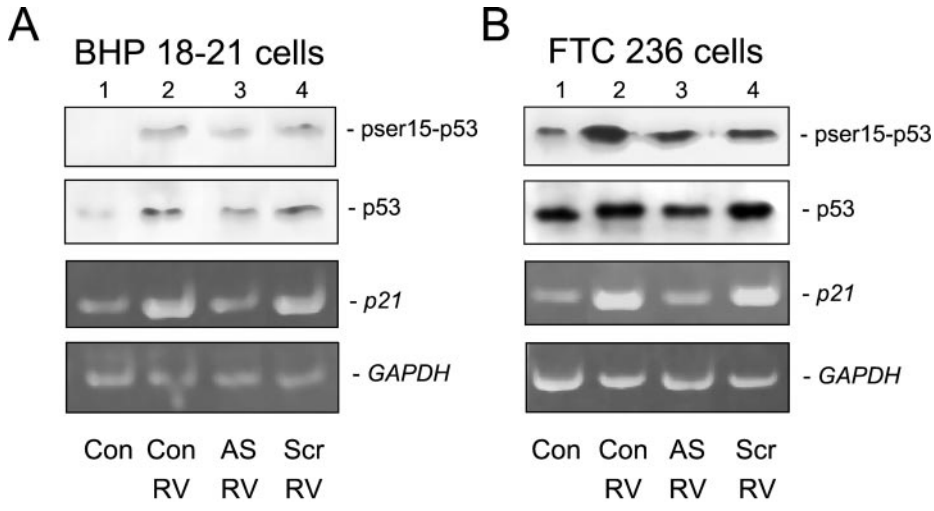

FIG. 6. Effect of *p53* antisense transfection on the nuclear accumulation of p53, phosphorylation of serine-15 of p53 and *p21* expression induced by RV. A, BHP 18–21 cells were transfected with *p53* Scr, AS, or no oligonucleotide (Con), then treated with RV (10 μM, 2 d). RV induced nuclear p53 accumulation and serine-15-p53 phosphorylation in Con cells (lane 2) and Scr cells (lane 4), but this effect was diminished in AS cells (lane 3). *p21* mRNA was increased in Con and Scr cells treated with RV (lanes 2 and 4) but this response was suppressed in AS cells (lane 3). B, A representative study in FTC 236 cells showed similar results, with increased nuclear p53 and pser15-p53 evident with RV in Con and Scr cells (lanes 2 and 4, respectively) and diminished responses to RV in AS cells (lane 3). The *p21* mRNA level increased with RV in Con and Scr cells (lanes 2 and 4), but not in AS cells (lane 3).

tent in cells. The abundance of p53 and expression of *p21* mRNA induced by RV were diminished by antisense but not by scrambled oligonucleotide transfection in BHP18–21 cells (Fig. 6A, lanes 3). Similar results were also observed in FTC 236 cells (Fig. 6B). These results with PFT-α and *p53* antisense oligonucleotide transfection strongly suggest that the expression of *p21* induced by RV is p53-dependent.

Role of MAPK in p53 phosphorylation and c-Fos and c-Jun expression induced by RV

To demonstrate that activated MAPK (ERK1/2) is essential for the action of p53, cells were treated with RV in the presence or absence of PD 98059 (PD), a specific MEK inhibitor (24). Results indicated that PD blocked the activation and nuclear translocation of ERKs 1 and 2 induced by RV in BHP 2–7 and BHP 18–21 thyroid cancer cell lines (Fig. 7A, lanes 4 compared with lanes 3). The phosphorylation of serine 15 on p53 induced by RV was inhibited by PD (Fig. 7A). There was no detectable serine 6 phosphorylation induced by RV (results not shown). c-Fos expression, stimulated by RV (lanes 3), was also inhibited by PD (lanes 4). *p53* mRNA did not change significantly with RV treatment (2 d) in BHP 2–7 cells, but c-*fos* mRNA increased with RV, an effect inhibited by PD (Fig. 7B). On the other hand, *p53* and c-*fos* mRNA increased with RV treatment in BHP 18–21 cells, an effect diminished by PD (Fig. 7B).

The inhibitory effect of PD on RV-induced p53 and MAPK activation and appearance of c-Fos was also observed in FTC 236 and FTC 238 cells (Fig. 8A). Phosphorylation of serines 6 and 15 on p53 was only minimally reduced by the MEK inhibitor in both follicular cancer cell lines (Fig. 8A). RV-induced *p53* mRNA in FTC 236 and FTC 238 cells was not appreciably affected by PD (lanes 4, Fig. 8B). Induction of c-*fos* and c-*jun* mRNA by RV (lanes 3) was reduced by addition of PD to these FTC cells (lanes 4).

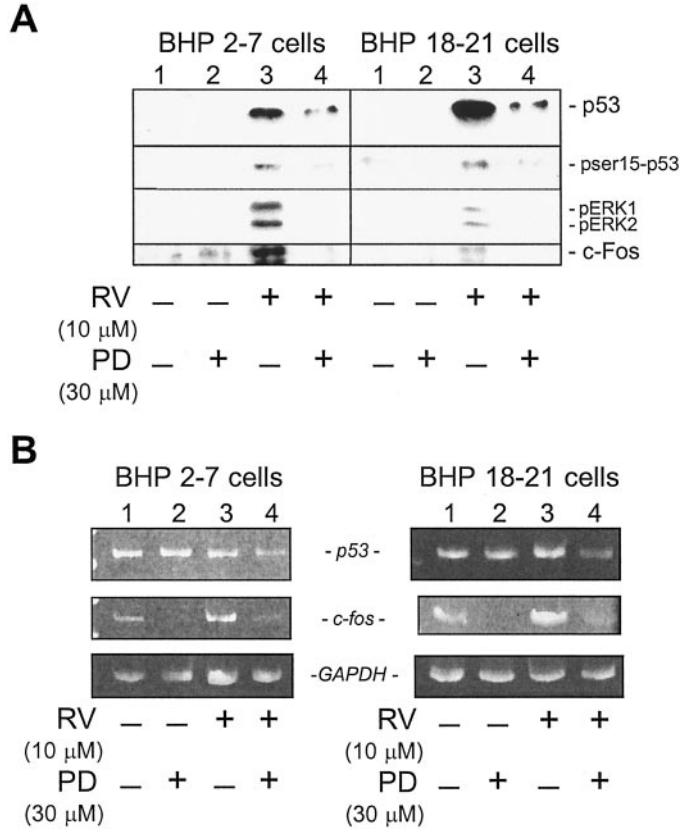

FIG. 7. Effect of PD98059 (PD) on RV-induced effects in BHP 2–7 and BHP 18–21 cells. A, RV treatment (10 μM, 2 d) caused nuclear accumulation of p53, serine 15-phosphorylated p53 (pser15-p53), phosphorylated ERKs 1 and 2 and c-Fos (lanes 3). This RV effect was blocked by PD (30 μM, 2 d). B, An increase in c-*fos* mRNA was seen with RV in both cell lines (lanes 3), which was inhibited by PD (lanes 4). A decrease in *p53* mRNA in cells treated with RV and PD was also noted.

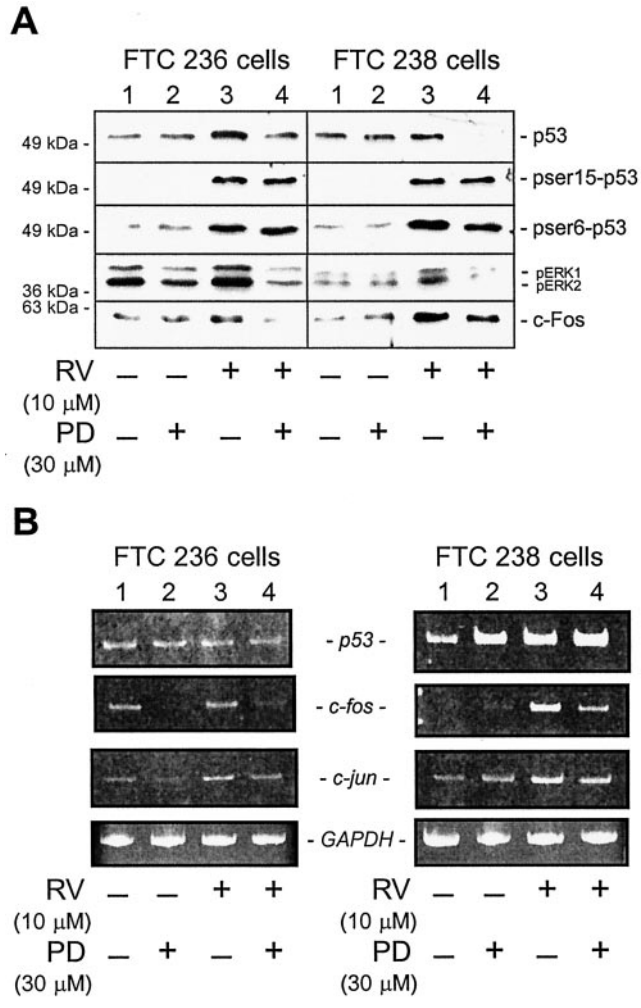

FIG. 8. Effect of PD on RV-induced p53 accumulation and phosphorylation, activated MAPK (pMAPK), *p53*, c-*fos*, and c-*jun* mRNA levels in FTC 236 and FTC 238 cells. A, RV treatment for 2 d caused accumulation of p53, pMAPK (ERK 1/2) and c-Fos (lanes 3). These effects were inhibited by PD (lane 4). Also increased by RV were serine-6- and serine-15-phosphorylated p53 (pser6-p53, pser15-p53). Formation of these phosphoproteins was partially inhibited by PD. B, An increase in c-*fos* and c-*jun* mRNAs was seen with RV (lanes 3), which was inhibited by PD (lane 4).

The role of ERK1/2 in the activation of p53 by RV in thyroid cancer cells was further confirmed by using *H-ras* antisense oligonucleotide transfection. The presence of antisense H-*ras* inhibited RV-induced ERK1/2 activation in BHP 2–7 and FTC 238 cells (Fig. 9, A and B, lanes 5 *vs.* 4). In cells transfected with a scrambled oligonucleotide (lanes 6), the response to RV was the same as in untransfected cells (lanes 4). The phosphorylation of serine 15 of p53 in BHP 2–7 and FTC 238 cells was also inhibited by *H-ras* antisense transfection (Fig. 9, A and B, lanes 5). FTC 238 cells displayed serine 6 phosphorylation of p53 in response to RV, which was inhibited by *H-ras* antisense transfection (Fig. 9B), but BHP 2–7 cells did not show serine 6 phosphorylation in response to RV. A similar lack of serine 6 phosphorylation was found with BHP 18–21 cells, whereas the response of FTC 236 cells resembled that of FTC 238 cells (results not shown). Not only the abundance and phosphorylation of p53 protein, but also the increase of *p53* and *p21* mRNA caused by RV (Fig. 9, C and D, lanes 4) were inhibited by *H-ras* antisense oligonucleotide transfection in BHP 2–7 and FTC 238 cells (lanes 5). These results demonstrate that activation of ERK1/2 by RV is Ras-dependent, and that a reduction in Ras affects serine phosphorylation of p53 and abundance of *p53* and *p21* mRNA in cells treated with RV.

Activated MAPK and phosphorylated p53 cooperatively induce apoptosis

RV caused increased nucleosome content indicating apoptosis in two papillary thyroid carcinoma cell lines, BHP 2–7 and BHP 18–21, and two follicular thyroid cancer cell lines, FTC 236 and FTC 238 (Fig. 10). When cells were treated with RV in the presence of PD, apoptosis was inhibited.

When cells were treated with RV in the presence of PFT-α, apoptosis was inhibited in BHP 2–7 and BHP 18–21 cells, as well as in FTC 236 and FTC 238 cells (Fig. 11). With the use of p53 antisense oligonucleotide transfection, we further confirmed the p53-dependence of RV-induced apoptosis in the same thyroid cancer cell lines (Fig. 12).

The nucleosome ELISA results were supported further by studies of DNA fragmentation, which showed that such fragmentation, induced by RV in both BHP 2–7 and FTC 236 cells, was blocked by PD and by *H-ras* antisense oligonucleotide transfection (Fig. 13, A and B). These results again support an essential role for the H-Ras-MEK-MAPK signaling pathway in p53-dependent apoptosis induced by RV.

Discussion

In the present studies, treatment of human thyroid cancer cells with the naturally occurring polyphenol, RV, disclosed the presence of *inducible* MAPK, and that such induction was associated with subsequent apoptosis. RV in low concentrations (1 pM-10 μM) has been reported by others to activate MAPK in human neuroblastoma SH-SY5Y cells (31), although higher concentrations (50–100 μM) of the stilbene inhibited MAPK activity in this cell line (31) and in other cells (32). In the studies described above, some activation of ERK1/2 was apparent in papillary and follicular thyroid cancer cells cultured for 3–5 d in the absence of RV, and exposure of these cells to RV resulted in further accumulation of these activated kinases. The RV effect was time- and concentration dependent. Activation of ERK1/2 by RV was blocked by either *H-ras* antisense oligonucleotide transfection or the MEK inhibitor, PD 98059. Thus, a Ras- and MEK-dependent signal transduction cascade is implicated in biologically-relevant activation of MAPK in these cells.

Other laboratories have proposed that constitutively active MAPK is required for maintenance of the malignant state, but that short-term activation of MAPK may direct cells to apoptosis (33). However, constitutive activation of MAPK in such studies may be a response of cell exposure to culture conditions for several days, as Fig. 1 in the present report suggests. What is clear, however, is that the modest activation of MAPK in *control* cells in our studies after 3–5 d in culture did not lead to activation of p53 and to apoptosis. It has been suggested by others that short-term activation of

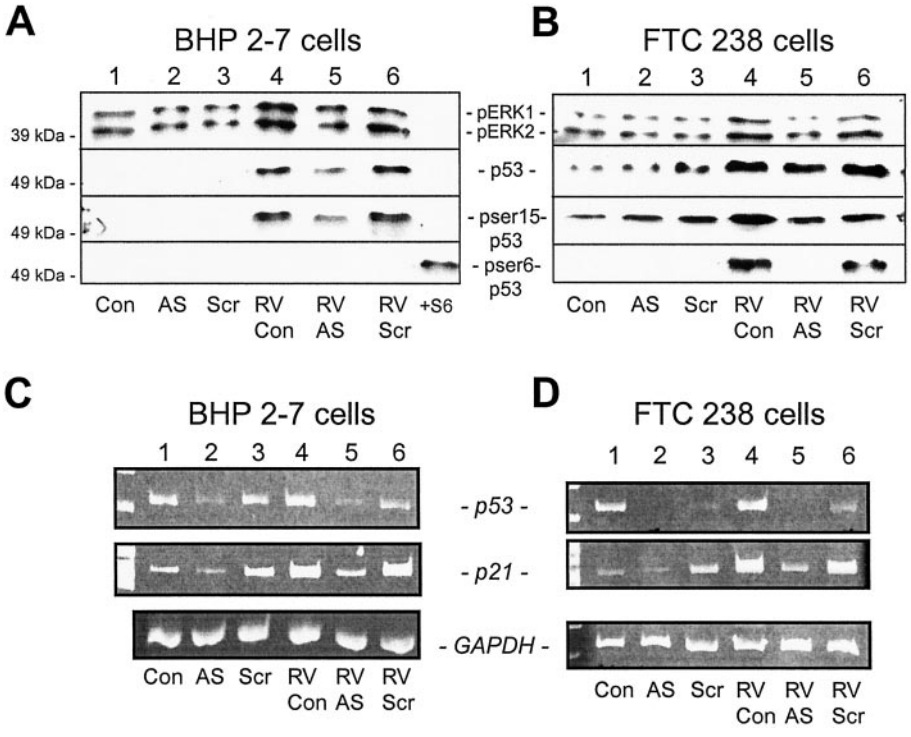

FIG. 9. Effect of *H-ras* antisense transfection on the activation of MAPK and p53, and p53 and p21 expression induced by RV. A, BHP 2–7 cells were transfected with *H-ras* Scr, AS, or no oligonucleotide (Con), and treated with RV (10 μM, 2 d). Nuclei were examined for levels of activated ERKs 1 and 2, p53, serine-15-phosphorylated p53 (pser15-p53) and serine-6-phosphorylated p53 (pser6-p53) by immunoblot. In a representative study, RV induced nuclear p53 accumulation and serine-15-p53 phosphorylation in Con cells (lanes 4 compared with lanes 1) and Scr cells (lanes 6 compared with lanes 3), but the RV effect was diminished in AS cells (lanes 5 compared with lanes 2). BHP 2–7 cells did not manifest any pser6-p53 before or after RV treatment (lanes 1–6). (+S6 indicates a positive control immunoblot for pser6-p53). B, A parallel study in FTC 238 cells showed similar results, with increased nuclear activated ERK1/2, p53 and pser15-p53 evident with RV in Con and Scr cells (lanes 4 and 6, respectively) and diminished responses to RV in AS cells (lanes 5). FTC 238 cells did show RV-induced p53 phosphorylation on serine 6 (Con and Scr cells, lanes 4 and 6), but the effect was blocked in AS cells (lane 5). C, In BHP 2–7 cells mRNAs for *p53* and *p21* were increased in Con cells treated with RV (lanes 4), but this response was suppressed in AS cells (lanes 5). D, Similar results were obtained in FTC 238 cells: AS cells treated with RV did not show marked increases in *p53* or *p21* mRNA (lanes 5) compared with responses in Con cells (lanes 4).

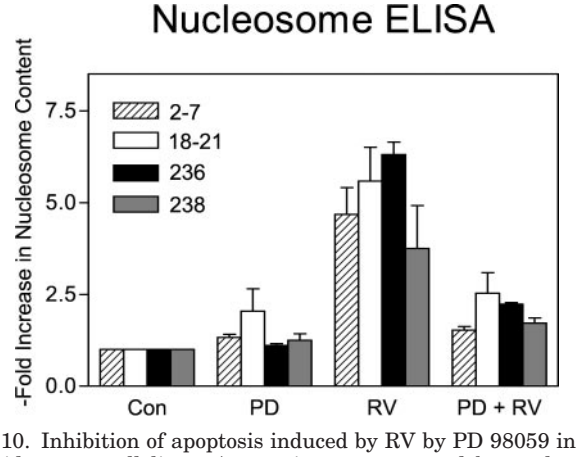

FIG. 10. Inhibition of apoptosis induced by RV by PD 98059 in four thyroid cancer cell lines. Apoptosis was measured by nucleosome ELISA in cells treated with RV (10 μM, 2 d), PD (30 μM, 2 d), or both agents. RV caused 3- to 6-fold increases in nucleosome content in the 4 cell lines, indicating apoptosis, and this effect was inhibited by cotreatment with PD (PD + RV). PD alone had no significant effect on apoptosis.

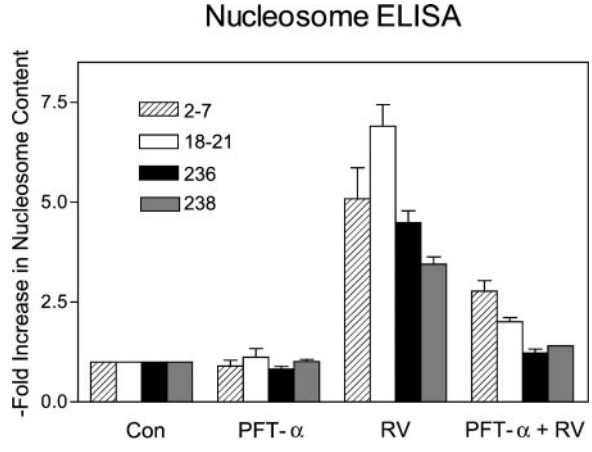

FIG. 11. Effect of the p53 inhibitor, PFT-α, on apoptosis in RV-treated cells, measured by nucleosome ELISA. Apoptosis induced by RV was inhibited by PFT-α in four thyroid cancer cell lines. Cells were treated with RV (10 μM, 2 d), PFT-α (20 μM, 2 d), or both agents. RV alone caused apoptosis, and PFT-α partially or completely inhibited RV-induced apoptosis in all thyroid cancer cell lines.

MAPK may be required for induction of apoptosis in normal cells (21).

Normal p53 function is essential to the induction of apoptosis in human and murine cells subjected to DNA damage (10). In some cancer and leukemic cells, high levels of p53 are found (16) but reflect the presence of dysfunctional, usually

mutated, protein. Apoptosis does not occur in such cells in response to the constitutively expressed p53. In the untreated follicular and papillary thyroid carcinoma cell lines we studied, low-to-moderate amounts of p53 were present constitutively, but apoptosis was not detected unless the cells were exposed to RV. The p53 that was transiently induced by RV appeared to retain function of the wild-type protein, in that its appearance was associated with immediate-early gene product accumulation and with apoptosis. By using an inhibitor of p53-dependent transcriptional activation, PFT-α, and p53 antisense oligonucleotide transfection, to block both RV-induced increase in abundance of p53 (Figs. 5 and 6) and RV-induced apoptosis (Figs. 11 and 12), we substantiated a role for p53 in promotion by RV of apoptosis in these thyroid cancer cells.

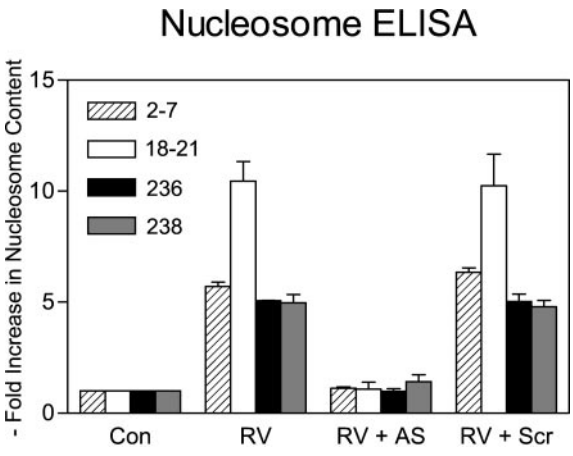

FIG. 12. Apoptosis induced by RV was inhibited by *p53* antisense oligonucleotide transfection in thyroid cancer cells. Four thyroid cancer cell lines were transfected with *p53* Scr, AS, or no oligonucleotide (Con), and treated with RV (10 μM, 2 d). Apoptosis was measured by nucleosome ELISA. *p53* AS transfection inhibited RV-induced apoptosis in all thyroid cancer cell lines.

RV (10–100 μM) induces apoptosis in several cancer cell models, including prostate cancer (4), breast cancer (34, 35), lymphoblasts (3), and leukemia (5). The present studies show for the first time that papillary and follicular thyroid cancer cell lines have an apoptotic response to RV. Huang *et al.* (3) have described RV-induced apoptosis in embryonic fibroblasts that express wild-type p53, but not in p53-deficient cells. Basolo and co-workers (17) have reported that expression of (presumptively wild-type) p53 is correlated with diversion of cells to apoptosis in papillary thyroid cancer. The present studies involving RV are consistent with these observations. Because both the *H-ras* antisense and MEK inhibitor paradigms decreased activation of p53 and the induction of apoptosis, it is clear that the latter two steps are linked to the MAPK pathway. In addition, because both the MEK inhibitor (Figs. 7 and 8) and *H-ras* antisense paradigms (Fig. 9) decreased activation of p53 and the induction of apoptosis (Figs. 10 and 13), it is clear that the latter two steps are linked to the MAPK pathway and provide a Ras- and MAPK-related mechanism by which the stilbene can increase cellular content of p53.

Overexpression of p53 has been shown to induce c-*fos* expression in a manner that differs from p53 expression in response to potentially oncogenic growth factors, such as epidermal growth factor (36). p53-induced c-*fos* expression is relevant to apoptosis. As Figs. 2–4 in this report show, RV not

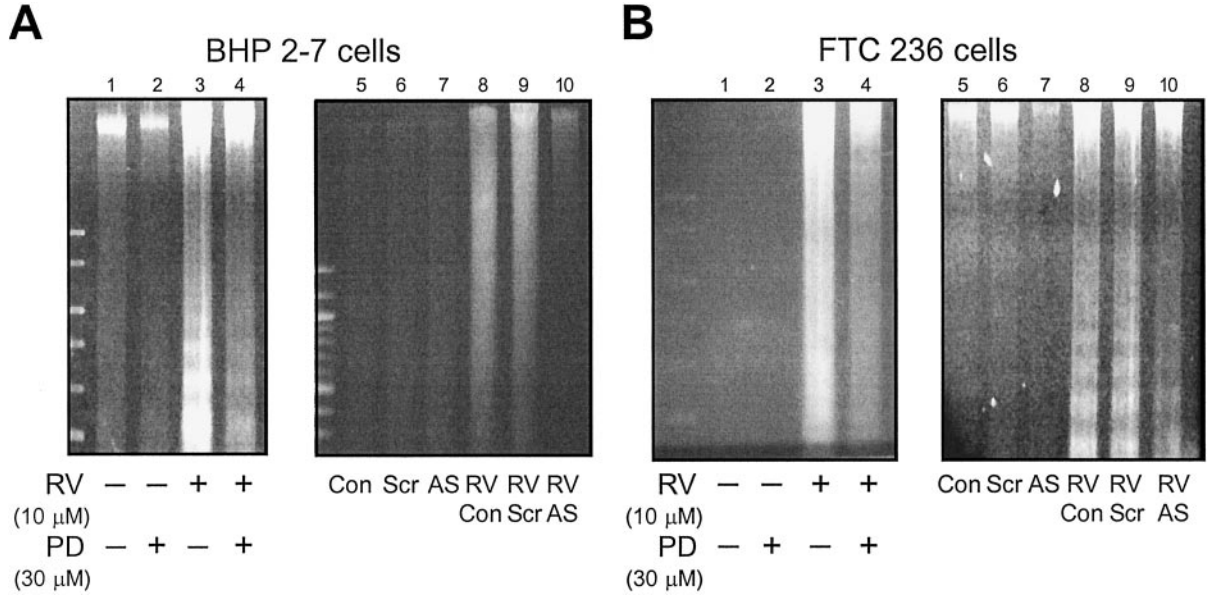

FIG. 13. RV-induced apoptosis in thyroid cancer cells, demonstrated by DNA fragmentation. A, BHP 2–7 cells were treated with RV (10 μM, 2 d), PD (30 μM, 2 d) or both, and DNA fragmentation determined as described in *Materials and Methods*. RV caused DNA laddering (lane 3), which was partially inhibited by PD (lane 4). In BHP 2–7 cells transfected with antisense (AS) *H-ras* oligonucleotide, RV-induced DNA fragmentation was reduced (lane 10), compared with findings in RV-treated cells transfected with scrambled oligonucleotide (Scr, lane 9), or cells not transfected (lane 8). B, FTC 236 cells were exposed to RV (10 μM, 2 d), PD (30 μM, 2 d) or both agents. RV treatment of these cells also caused DNA fragmentation (lane 3), which was partially inhibited by PD (lane 4). RV also caused apoptosis in untransfected cells (Con) and cells transfected with Scr oligonucleotide (lanes 8 and 9), but with AS *H-ras* transfection the cells were partially protected from apoptosis (lane 10).

only promoted accumulation of p53, but also of c-Fos and c-Jun, in thyroid cancer cells. The abundance of respective mRNAs of c-*fos* and c-*jun* was also increased in RV-treated cells.

Studies by Hsieh *et al.* (37) have also demonstrated that RV increases accumulation of cellular p53 and the cyclin-dependent protein kinase inhibitor, p21, in cultured pulmonary artery endothelial cells. p21 was originally identified as a transcriptional target of p53 (38). It is now known that this protein is a component of a complex containing cyclins, cyclin-dependent kinases and proliferating cell nuclear antigen (39). An increased amount of p21 in the quaternary complex leads to inhibition of DNA synthesis and cell cycle arrest (40) that permits DNA repair to proceed. In both papillary and follicular thyroid carcinoma cells, we also found that RV increased cellular abundance of p21 protein and mRNA (Figs. 2–6 and 9). This stilbene-dependent increase in *p21* mRNA was reduced by cell treatment with the p53-specific inhibitor, PFT-α (Fig. 5) and p53 antisense oligonucleotide transfection (Fig. 6), suggesting that RV-induced *p21* expression is p53-dependent. These results are consistent with a role for p21 in p53-dependent apoptosis that is caused by RV. RV-induced p53-dependent p21 expression was inhibited by *H-ras* antisense oligonucleotide treatment (Fig. 9) and corresponded to a reduction in RV-induced apoptosis (Fig. 13), further solidifying the connection between MAPK and p53 signals.

Phosphorylation of p53 determines the biological activity of the protein. At several serine residues, including serine 6 and serine 15, phosphorylation has been shown to be relevant to DNA damage (10) and apoptosis (41). In our studies, there were differences between papillary and follicular thyroid cancer cells in the serine phosphorylation patterns caused by RV. That is, both serine 6 and serine 15 were phosphorylated in follicular cancer cells treated with RV, but serine 6 was not phosphorylated in papillary cancer cells. However, serine phosphorylation-dependent apoptosis was induced by RV in both cell types. Stilbene-related serine 15 phosphorylation in papillary thyroid cancer cells was inhibited by PD 98059 to a greater extent than in follicular thyroid cancer cells, but the *H-ras* antisense oligonucleotide paradigm was highly effective in all cancer cell lines in blocking serine 15 phosphorylation of p53. RV-induced serine 6 phosphorylation in follicular thyroid cancer cells was minimally affected by PD 98059 but was completely inhibited by antisense *H-ras* transfection under conditions of these experiments. This suggests that the mechanism of RV-induced phosphorylation of p53 involves MAPK at serine 15, but another serine kinase at residue 6. As noted above, p53 is also a substrate for JNK (13) and p38 kinase (14). It is not clear how relevant serine 6 phosphorylation is to apoptosis (41), and in the present studies we show that serine 6 phosphorylation by RV is not required in papillary thyroid cancer cells for apoptosis to occur.

Acknowledgments

Drs. J. Hershman and O. Clark kindly provided thyroid cancer cell lines for study.

Received September 10, 2001. Accepted December 10, 2001.

Address all correspondence to: Hung-Yun Lin, Ph.D., Clinical Research Institute MC-16, Albany Medical College, Albany, New York 12208. E-mail: linhungyun@hotmail.com. Address all requests for reprints to: Dr. Paul J. Davis, Clinical Research Institute, MC-16, Albany Medical College, 47 New Scotland Avenue, Albany, New York 12208.

This work was supported in part by the Office of Research Development, Medical Research Service, Department of Veterans Affairs (to P.J.D.), and grants from the Candace King Weir Foundation and the Charitable Leadership Foundation.

References

1. **Jayatilake GS, Jayasuriya H, Lee ES, Koonchanok N M, Geahlen RL, Ashendel CL, McLaughlin JL, Chang CJ** 1993 Kinase inhibitors from *Polygonum cuspidatum*. J Nat Prod 56:1805–1810
2. **Jang M, Cai L, Udeani GO, Slowing KV, Thomas CF, Beecher CW, Fong HH, Farnsworth NR, Kinghorn AD, Mehta RG, Moon RC, Pezzuto JM** 1997 Cancer chemopreventive activity of resveratrol, a natural product derived from grapes. Science 275:218–220
3. **Huang C, Ma WY, Goranson A, Dong Z** 1999 Resveratrol suppresses cell transformation and induces apoptosis through a p53-dependent pathway. Carcinogenesis (Lond) 20:237–242
4. **Hsieh TC, Wu JM** 1999 Differential effects on growth, cell cycle arrest, and induction of apoptosis by resveratrol in human prostate cancer cell lines. Exp Cell Res 249:109–115
5. **Clement M-V, Hirpara JL, Chawdhury SH, Pervaiz S** 1998 Chemopreventive agent resveratrol, a natural product derived from grapes, triggers CD95 signaling-dependent apoptosis in human tumor cells. Blood 92:996–1002
6. **Tsan M-F, White JE, Maheshwari JG, Bremner TA, Sacco J** 2000 Resveratrol induces Fas signalling-independent apoptosis in THP-1 human monocytic leukaemia cells. Brit J Haematol 109:405–412
7. **White K, Grether ME, Abrams JM, Young L, Farrell K, Steller H** 1994 Genetic control of programmed cell death in Drosophila. Science 264:677–683
8. **Martin SJ, Green DR** 1995 Protease activation during apoptosis: death by a thousand cuts? Cell 82:349–352
9. **Sen S, D'Incalci M** 1992 Apoptosis. Biochemical events and relevance to cancer chemotherapy. FEBS Lett 307:122–127
10. **Higashimoto Y, Saito S, Tong XH, Hong A, Sakaguchi K, Appella E, Anderson CW** 2000 Human p53 is phosphorylated on serines 6 and 9 in response to DNA damage-inducing agents. J Biol Chem 275:23199–23203
11. **Ashcroft M, Kubbutat MHG, Vousden KH** 1999 Regulation of p53 function and stability by phosphorylation. Mol Cell Biol 19:1751–1758
12. **Agarwal ML, Taylor WR, Chernov MV, Chernova OB, Stark GR** 1998 The p53 network. J Biol Chem 273:1–4
13. **Fuchs SY, Adler V, Pincus MR, Ronai Z** 1998 MEKK1/JNK signaling stabilizes and activates p53. Proc Natl Acad Sci USA 95:10541–10546
14. **She QB, Chen N, Dong Z** 2000 ERKs and p38 kinase phosphorylate p53 protein at serine 15 in response to UV radiation. J Biol Chem 275:20444–20449
15. **Mashimo T, Bandyopadhyay S, Goodarzi G, Watabe M, Pai SK, Gross SC, Watabe K** 2000 Activation of the tumor metastasis suppressor gene, KAI1, by etoposide is mediated by p53 and c-Jun genes. Biochem Biophy Res Commun 274:370–376
16. **Itaya M, Yoshimoto J, Kojima K, Futagawa S** 1999 Usefulness of p53 protein, Bcl-2 protein and Ki-67 as predictors of chemosensitivity of malignant tumors. Oncol Rep 6:675–682
17. **Basolo F, Pollina L, Fontanini G, Fiore L, Pacini F, Baldanzi A** 1997 Apoptosis and proliferation in thyroid carcinoma: correlation with bcl-2 and p53 protein expression. Brit J Cancer 75:537–541
18. **Ostrowski J, Trzeciak L, Kolodziejski J, Bomsztyk K** 1998 Increased constitutive activity of mitogen-activated protein kinase and renaturable 85 kDa kinase in human-colorectal cancer. Brit J Cancer 78:1301–1306
19. **Kim SC, Hahn JS, Min YH, Yoo NC, Ko YW, Lee WJ** 1999 Constitutive activation of extracellular signal-regulated kinase in human acute leukemias: combined role of activation of MEK, hyperexpression of extracellular signal-regulated kinase, and downregulation of a phosphatase, PAC1. Blood 93: 3893–3899
20. **Chen Z, Sun J, Pradines A, Favre G, Adnane J, Sebti SM** 2000 Both farnesylated and geranylgeranylated RhoB inhibit malignant transformation and suppress human tumor growth in nude mice. J Biol Chem 275:17974–17978
21. **Ishikawa Y, Kitamura M** 1999 Dual potential of extracellular signal-regulated kinase for the control of cell survival. Biochem Biophys Res Commun 264: 696–701
22. **Pavlovic D, Andersen NA, Mandrup-Poulsen T, Zizirik DL** 2000 Activation of extracellular signal-regulated kinase (ERK)1/2 contributes to cytokine-induced apoptosis in purified rat pancreatic beta-cells. Eur Cytokine Netw 11:267–274
23. **Persons DL, Yazlovitskaya EM, Pelling JC** 2000 Effect of extracellular signal-regulated kinase on p53 accumulation in response to cisplatin. J Biol Chem 275:35778–35785

24. **Shih A, Lin H-Y, Davis FB, Davis PJ** 2001 Thyroid hormone promotes serine phosphorylation of p53 by mitogen-activated protein kinase. Biochemistry 40:2870–2878
25. **Xu XS, Vanderziel C, Bennett CF, Monia, BP** 1998 A role for c-Raf kinase and Ha-Ras in cytokine-mediated induction of cell adhesion molecules. J Biol Chem 273:33230–33238
26. **Mahdi T, Brizard A, Millet C, Dore P, Tanzer J, Kitzis A** 1995 *In vitro* p53 and/or Rb antisense oligonucleotide treatment in association with growth factors induces the proliferation of peripheral hematopoietic progenitors. J Cell Sci 108:1287–1293
27. **Lin H-Y, Martino LJ, Wilcox BD, Davis FB, Davis PJ** 1998 Potentiation by thyroid hormone of human IFN-γ-induced HLA-DR expression. J Immunol 161:843–849
28. **Irving J, Feng J, Wistrom C, Pikaart M, Villeponteau B** 1992 An altered repertoire of fos/jun (AP-1) at the onset of replicative senescence. Exp Cell Res 202:161–166
29. **Potapova D, Gorospe M, Dougherty RH, Dean NM, Gaarde WA, Holbrook NJ** 2000 Inhibition of c-Jun N-terminal kinase 2 expression suppresses growth and induces apoptosis of human tumor cells in a p53-dependent manner. Mol Cell Biol 20:1713–1722
30. **Komarov PG, Komarova EA, Kondratov RV, Christov-Tselkov K, Coon JS, Chernov MV, Gudkov AV** 1999 A chemical inhibitor of p53 that protects mice from the side effects of cancer therapy. Science 285:1733–1737
31. **Miloso M, Bertelli AA, Nicolini G, Tredici G** 1999 Resveratrol-induced activation of the mitogen-activated protein kinases, ERK1 and ERK2, in human neuroblastoma SH-SY5Y cells. Neurosci Lett 264:141–144
32. **El-Mowafy AM, White RE** 1999 Resveratrol inhibits MAPK activity and nuclear translocation in coronary artery smooth muscle: reversal of endothelin-1 stimulatory effects. FEBS Lett 451:63–67
33. **Lassus P, Roux P, Zugasti O, Philips A, Fort P, Hibner U** 2000 Extinction of rac1 and Cdc42Hs signalling defines a novel p53-dependent apoptotic pathway. Oncogene 19:2377–2385
34. **Mgbonyebi OP, Russo J, Russo IH** 1998 Antiproliferative effect of synthetic resveratrol on human breast epithelial cells. Int J Oncol 12:865–869
35. **Lu R, Serrero G** 1999 Resveratrol, a natural product derived from grape, exhibits antiestrogenic activity and inhibits the growth of human breast cancer cells. J Cell Physiol 179:297–304
36. **Elkeles A, Juven-Gershon T, Israeli D, Wilder S, Zalcenstein A, Oren M** 1999 The c-fos proto-oncogene is a target for transactivation by the p53 tumor suppressor. Mol Cell Biol 19:2594–2600
37. **Hsieh TC, Juan G, Darzynkiewicz Z, Wu JM** 1999 Resveratrol increases nitric oxide synthase, induces accumulation of p53 and p21(WAF1/CIP1), and suppresses cultured bovine pulmonary artery endothelial cell proliferation by perturbing progression through S and G2. Cancer Res 59:2596–2601
38. **El-Deiry W.S, Tokino T, Velculescu VE, Levy DB, Parsons R, Trent JM, Lin D, Mercer WE, Kinzler KW, Vogelstein B** 1993 WAF1, a potential mediator of p53 tumor suppression. Cell 75:817–825
39. **Chen J, Jackson PK, Kirschner MW, Dutta A** 1995 Separate domains of p21 involved in the inhibition of Cdk kinase and PCNA. Nature 374:386–388
40. **Harper JW, Adami GR, Wei N, Keyomarsi K, Elledge SJ** 1993 The p21 Cdk-interacting protein Cip1 is a potent inhibitor of G1 cyclin-dependent kinases. Cell 75:805–816
41. **Unger T, Sionov RV, Moallem E, Yee CL, Howley PM, Oren M, Haupt Y** 1999 Mutations in serines 15 and 20 of human p53 impair its apoptotic activity. Oncogene 18:3205–3212